11th World Congress on Structural and Multidisciplinary Optimisation
07th -12th, June 2015, Sydney Australia

Elimination of void element influence on optimization for nonlinear compliance with a buckling constraint using moving iso-surface threshold method

Liyong Tong[1], Quantian Luo[2]

[1] School of Aerospace, Mechanical and Mechatronic Engineering, The University of Sydney, Sydney, NSW 2006, Australia, liyong.tong@sydney.edu.au
[2] School of Aerospace, Mechanical and Mechatronic Engineering, The University of Sydney, Sydney, NSW 2006, Australia, quantian.luo@sydney.edu.au

Abstract

This article presents an algorithm that eliminates some of the adverse influences of the void elements used in nonlinear structural topology optimization with a buckling constraint by using moving iso-surface threshold (MIST) method. The basic idea of this algorithm is to conduct the finite element analysis in a sub design domain with solid and grey elements and to construct each updated response function in the full design domain. In this algorithm, void elements are excluded in all the finite element analyses but included in design variable update. In doing so in MIST, the material removed with void elements can reappear. In the present study, the strain energy density at the final state in a nonlinear finite element analysis is selected as the response function in MIST to minimize the nonlinear compliance, and the iso-surface threshold value is determined by using a prescribed volume constraint and then used to define optimal topology containing solid materials only. Exclusion of void elements in all the finite element analyses allows avoidance of several numerical issues, such as material reappearance, discontinuous design and numerical instability encountered in topology optimization for structures, in particular, with large displacements. In the present algorithm, a buckling constraint is also introduced to consider the influence of load level on nonlinear topology optimization.

Keywords: optimization, nonlinearity, void element, numerical stability, buckling constraint

1. Introduction

It is known that the inclusion of large displacements in topology optimizations, for example, to minimize the structural compliance, can significantly affect the final designs and serious numerical issues were encountered in nonlinear topology optimizations owing to the use of void elements [1-6]. These issues include: 1) the geometrically nonlinear finite element analysis (FEA) is hardly convergent to the full level of an applied loading state due to excessively large displacements caused by rather low stiffness of the void elements; 2) the convergence is poor as the excessively large displacements cause mesh distortions which in turn deteriorate the displacement fields; and 3) numerical instabilities can occur in a localized region with a cluster of void elements so that the obtained topology may not be well defined and practical. Therefore, an adequate treatment of the void elements is essential in order to effectively conduct topology optimization for geometrically nonlinear structures.

A number of methods have been proposed to attempt to circumvent the influences of void elements in topology optimization problem to minimize nonlinear compliance. One direct approach to completely solve the issues is to remove all void elements. However, this creates other issues, e.g. material reappearance, disconnected or disjointed structure and design domain re-meshing. This study aims to develop an effective algorithm that resolves these issues by excluding all void elements in FEA and including all of them in design updates.

As the optimum topology obtained via minimizing the nonlinear compliance can be highly dependent on the level of the applied loads, in this paper, we propose a novel algorithm by introducing a buckling constraint in which the applied load varied with iteration is constrained by the critical buckling factor. This is because buckling is one of the most serious structural failure mechanisms, particularly for the optimized structures as they are often thin-walled, therefore the introduction of the buckling constraint in general form is also important in topology optimization.

For topology optimization problems involving buckling, there also exist severe numerical difficulties due to the adverse effects of low density and void elements [7-13]. In the present novel algorithm, these adverse influences can also be eliminated effectively via the exclusion and inclusion of all void elements in FEA and design updates.

2. Problem statement

Let us consider the minimum mean compliance problem for nonlinear structures. To use MIST [14], the nonlinear compliance needs to be expressed in an integral form. When the external loads are expressed as a function of time t_n and the total Lagrangian formulation is used to describe the equilibrium equations in ($t_n + \Delta t_n$), the nonlinear compliance can be expressed as:

$$C = \lim_{n\to\infty}\sum_{i=1}^{n}\left(\mathbf{F}_i^T + \mathbf{F}_{i-1}^T\right)\Delta\mathbf{u}_{i-1} = 2\int_0^{t_L}\mathbf{F}^T d\mathbf{u} = 2\lim_{n\to\infty}\sum_{i=0}^{n-1}\int_{\Omega_1}{}^{(t_n+\Delta t_n)}S_{ij}\delta\varepsilon_{ij}d\Omega = 2\int_{\Omega_1}\left(\int_0^{t_L}S_{ij}d\varepsilon_{ij}\right)d\Omega \tag{1a}$$

where $\{\mathbf{F}_i\}$ denotes the stress resultant vector in the state of time t_i; $\boldsymbol{u}$ is the displacement vector; t_L denotes a final equilibrium state with full loads; Ω_1 denotes design domain 1 that contains solid and grey elements only; S_{ij} and ε_{ij} are the Piola-Kirchhoff stress and the Green-Lagrange strain. For linearly elastic material, ${}_0^{t_n}S_{ij} = {}_0^{t_n}C_{ijkl}\,{}_0^{t_n}\varepsilon_{kl}$ and ${}_0^{t_n}C_{ijkl}$ is the constant tensor. Thus the nonlinear compliance can be defined as:

$$C = 2\int_{\Omega_1}\frac{1}{2}{}^{t_L}S_{ij}\,{}^{t_L}\varepsilon_{ij}d\Omega \tag{1b}$$

We now define the MIST formulation for the problem of minimizing nonlinear compliance with a buckling constraint as follows:

Minimize: C (2a)

$$\text{Subject to:}\begin{cases}\{\mathbf{R}(\mathbf{u},\mathbf{x_e})\} = 0 & \text{in } \Omega_1\\ \sum_{e=1}^{N_s}(x_e V_e) \le V_f V & \\ \overline{\lambda}_1 \ge 1 & \\ \text{Load path continuity in } \Omega_1 & \\ 0 \le x_e \le 1 & \end{cases} \tag{2b}$$

$$\Phi \text{ function:} \quad \Phi = \begin{cases}\frac{1}{2}{}^{t_L}S_{ij}\,{}^{t_L}\varepsilon_{ij} & \varepsilon < x_e \le 1 \quad \text{in } \Omega_1\\ 0 & 0 \le x_e \le \varepsilon \quad \text{in } \Omega_2\end{cases} \tag{2c}$$

where $\boldsymbol{x_e}$ denotes the design variables, e.g. representing solid ($x_e = 1$), grey ($\varepsilon < x_e < 1$) and void ($0 \le x_e \le \varepsilon$) elements; ε is the small parameter (e.g., $\varepsilon = 10^{-3}$); V_e and V represent volumes of element e and the design domain (Ω); V_f is the prescribed volume fraction; N_s is the number of solid and grey elements in domain 1 (Ω_1); Ω_2 is domain 2 with void elements only; N_e is the total element number; Φ denotes the response function; ${}^{t_L}S_{ij}$ and ${}^{t_L}\varepsilon_{ij}$ are the Piola-Kirchhoff stress and the Green-Lagrange strain in a final state with the full load; $\{\mathbf{R}\}$ is the residual force; $\overline{\lambda}_1$ is the buckling factor of mode 1.

The residual force $\{\mathbf{R}\}$ in the equilibrium equations and the buckling factor $\overline{\lambda}_1$ are defined as:

$$\{\boldsymbol{R}\} = \{\boldsymbol{F}\} - \{\boldsymbol{F_r}\} \tag{3}$$

$$\overline{\lambda}_1 P_n = P_{n-1} + \lambda_{n1}\varDelta P_n \tag{4}$$

where $\{\boldsymbol{F}\}$ is the external force vector; $\{\boldsymbol{F_r}\}$ denotes the stress resultant vector in the final state; F^k and u^k are the external force component and the corresponding displacement; N_F and N_L are numbers of force components and load increments; P_n represents the final state of load increments; P_{n-1} is the last 2nd load step; and λ_{n1} is the buckling factor of mode 1 due to load increment $\varDelta P_n$.

It is worth noting that equation (2b) shows that all FEA are conducted in Ω_1 and equation (2c) reveals that the response function Φ is constructed in Ω which enables design updates in full design domain.

3. An efficient MIST algorithm

The MIST involves finding and updating an iso-surface threshold value for the chosen response function subjected to a prescribed constraint. The objective function in MIST can be expressed as [14]:

$$J = \int_\Omega \Phi(x)H(t,\Phi(x))d\Omega \tag{5}$$

where $\Phi(x)$ is the response function; $H(t,\Phi(x))$ is the Heaviside function: $H(t,\Phi(x)) = 1$ for every x in the set of $\Phi(x) \ge t$, and $H(t,\Phi(x)) = 0$ for x in the set of $\Phi(x) < t$; Ω represents the full design domain. When the threshold level t is determined, the design variable x is defined by:

$$\begin{cases} \Phi(x) \geq t & \Leftrightarrow \quad x = 1 \\ \Phi(x) < t & \Leftrightarrow \quad x = 0 \end{cases} \tag{6}$$

where $x = 1$ and $x = 0$ represent solid and void at location x.

In the finite element based optimization, the response function is constructed using the nodal physical quantities and the material density x_e ($e = 1, 2 \dots N_e$) defined by the fraction of the solid material in element e are used as the design variables. At iteration k, $(x_e)_k^{(1)} = 1$ if $\Phi_k \geq t_k$ at all nodes of element e; $(x_e)_k^{(1)} = 0$ if $\Phi_k < t_k$ at all nodes and $(x_e)_k^{(1)} = A_{epj} / A_e$ when $\Phi_k \geq t_k$ at some nodes, where A_{epj} is the project area of the $\Phi(t_k)$ ($\geq t_k$) within the element. The design variables are updated by:

$$\{\mathbf{x}_e\}_k^{(2)} = \{\mathbf{x}_e\}_{(k-1)} + k_{mv}(\{\mathbf{x}_e\}_k^{(1)} - \{\mathbf{x}_e\}_{k-1}) \tag{7}$$

$$(x_e)_k^{(3)} = \begin{cases} (x_e)_k^{(2)} & (x_e)_k^{(2)} > \varepsilon \\ 0 & (x_e)_k^{(2)} \leq \varepsilon \end{cases} \qquad (e = 1, 2, \dots, N_e) \tag{8}$$

where k_{mv} is the move limit and $0 \leq k_{mv} \leq 1$.

A distinctive feature of the present MIST algorithm is the use of two meshes that facilitate element removal and reappearance easily. One mesh is fixed for the full design domain Ω used for constructing the Φ function and determining design variable updates, and the other is dynamic denoted Ω_1 with solid and grey elements only for conducting all FEA. As all void elements are excluded in the FEA, thus the associated adverse effects are completely eradicated. The re-meshing issue can be solved by renumbering the elements in Ω_1 and the material reappearance is automatically realized by using equations (2c), (7) and (8). Another feature of the MIST algorithm is that it can be easily interfaced with any commercially available FEA software. In this study, the MIST algorithm is interfaced with NASTRAN.

4. A MIST algorithm for including a buckling constraint

It is known that the topology optimization of geometrically nonlinear structures can rely on the magnitude of an applied load. This raises an issue which one is the optimal topology in a topology design optimization. We propose that the topology obtained by the maximum load without causing buckling be the optimum one. This can be defined by applying the buckling constraint as given in Eq. (2b).

By using the MIST, the optimization can be conducted by applying load:

$$P_k = \overline{\lambda}_1^{k-1} P_{k-1} \tag{9}$$

where P_{k-1} and P_k are the applied loads at iteration (k-1) and k; $\overline{\lambda}_1^{k-1}$ is the buckling factor in equation (4) at iteration (k-1).

As discussed in [9, 15], an accurate calculation of a linear buckling factor can be very difficult in topology optimization due to the impact of low density and void elements. It is even more difficult to accurately calculate the nonlinear buckling factor, as indicated by equation (4). Hence it is evident that the removal of all void elements is of paramount importance in solving design optimization problem, such as to minimize nonlinear structural compliance. An approach for the removal of void elements and material reappearance in MIST has been developed to minimize the nonlinear compliance of a structure with material and geometric nonlinearities [16]. This method is extended in this study to the topology optimization for minimum nonlinear compliance with the buckling constraint as the optimal design depends on the magnitude of the applied load.

When the material nonlinearity is not considered, the linear buckling factor may be used to reduce the computational cost as it is usually slightly larger than the nonlinear buckling factor, and hence it is used in this study for simplicity. When there is no buckling mode in an optimal structure, the maximum stress constraint may be introduced to obtain the optimal topology for the nonlinear compliance. In the early iterations, the buckling factor may be sharply altered due to the effects of low density elements. In practical computations, the buckling constraint can be introduced after certain number of iteration. In all the present computation, the buckling constraint is applied when the removal of void elements commences.

3. Numerical results and discussion

Numerical results are presented for the two samples shown in Figure 1 to illustrate the effectiveness of the present MIST algorithm for topology optimization of geometrically nonlinear structures.

3.1 Optimization for a specific load

Sample 1 of Figure 1(a) was studied in [17-19]. The data given in Figure 1(a) are the same as those in [19]. When F = 2 MN, the optimal topologies btained by using the present algorithm are illustrated in Figure 2(a) and 2(b), which are similar to those in [19]. However, the linear and nonlinear compliances predicted by the present computation are 24.5% and 9.64% lower than those (C* in Figure 2(a) and (b)) in [19]. Variations of the nonlinear compliance (C), the buckling factor (Eig_1) and the numbers of void (N_void) and solid (N-solid) elements are illustrated in Figure 2(c).

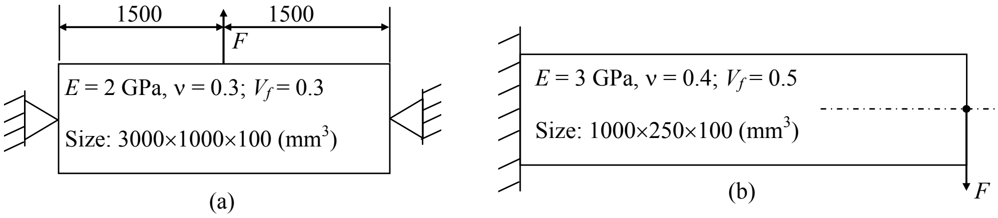

Figure 1 Design domains of samples 1 (mesh: 120×40) and 2 (mesh: 160×40)

Sample 2 in Figure 1(b) was investigated by many researchers [1, 2, 6, 19, 20]. When F = 144 kN, the optimal topologies obtained in the present computation are plotted in Figure 3, which collate well with those in [1]. The present linear and nonlinear compliances are 8.74% and 9.03% lower than those (C* in Figure 3) in [1].

Figures 2 and 3 show that the present nonlinear compliances are around 9% lower than those in the literature even though the topologies were similar; this could be due to the effects of the void elements on the accurate estimation of the nonlinear compliances. Figure 2(c) also indicates that the all the quantities converge almost within 30 iterations. Material distributions or densities at iterations 1, 5, 10 and 30 are given in Figure 4. It can be seen that the removal of void elements and material reappearance can be realized in the present computation. At iteration 30, C = 432.7 kJ, λ_1 = 6.402, N_void = 3214 and 1296; and at iteration 100, these data are 430.5 kJ, 6.418, 3234 and 1308, respectively. Figures 2(c) and 4 reveal a fast convergence rate of the present algorithm.

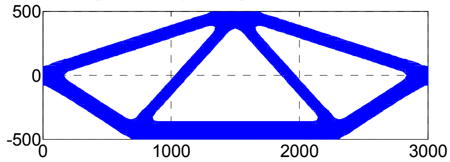

(a) C = 595 kJ (C* = 788 kJ)

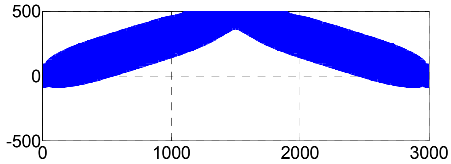

(b) C = 431 kJ (C* = 477 kJ)

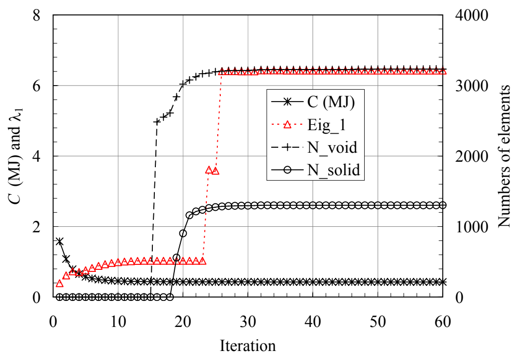

(c) Nonlinear compliance versus iteration

Figure 2 Optimization for sample 1: (a) optimal topology for linear analysis; (b) optimal design for nonlinear analysis; (c) nonlinear compliance and removal of void elements

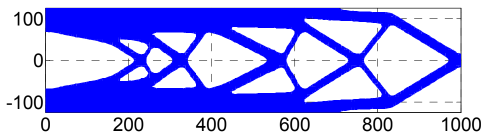

(a) C = 24.64 kJ (C* = 27.00 kJ)

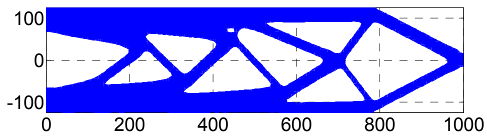

(b) C = 23.58 kJ (C* = 25.92 kJ)

Figure 3 Optimization for sample 2: (a) topology for linear analysis; (b) optimal design for nonlinear analysis

(a) Iteration = 1; C = 1579 kJ

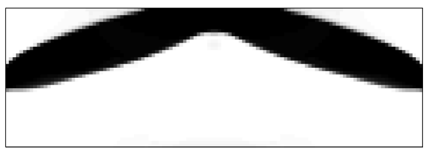

(c) Iteration = 10; C = 457.7 kJ

(b) Iteration = 5; C = 577.8 kJ

(d) Iteration = 30; C = 432.7 kJ

Figure 4 Material distributions at iterations 1, 5, 10 and 30

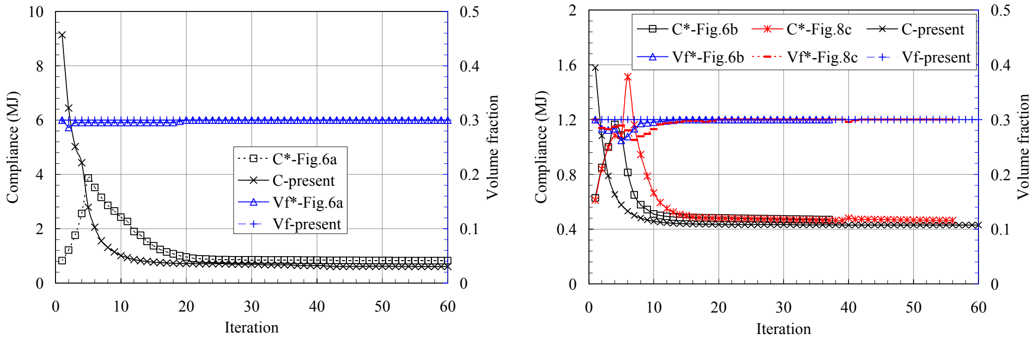

(a) linear analysis (b) nonlinear analysis

Figure 5 A comparison of the compliances predicted by the MIST and SIMP [19](quantities with asterisks)

A comparison of the compliance versus iteration curves for linear and nonlinear cases computed by the present algorithm and in [19] is illustrated in Figure 5. It is evident that the numerical stability, convergence performance and the minimum compliances of the present computation appear better than those in [19] where the SIMP was used by combining a meshless method with a density interpolation to treat void elements.

For the cases of F = -10 kN and F = -1 MN, the present optimal designs are plotted in Figure 6. It is obvious that the two designs are different. Different designs were also observed for different load levels in [1] for sample 2. That is, topologies can be dependent on the load levels in optimization for nonlinear compliance. In the present algorithm, the buckling constraint is used to find the optimal designs.

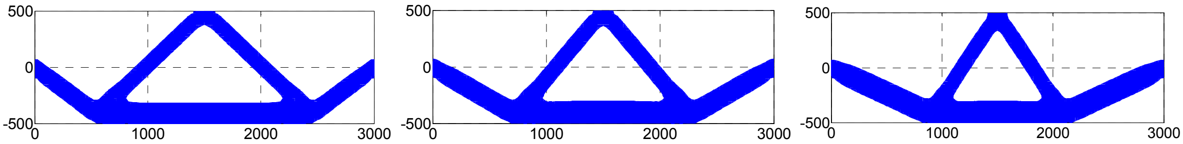

(a) F = - 10 kN; C = 14.1 J (b) F = -1 MN; C = 163 kJ (c) F = -1.445 MN; C = 277 kJ

Figure 6 Optimization for nonlinear compliance of sample 1

3.2 Optimal design with buckling constraint

In the present iteration process, equation (9) is applied when the removal of void elements starts. The optimal topology to minimize the nonlinear compliance for sample 2 predicted by the present algorithm is shown in Figure 6(c), which is different from those in Figure 6(a) or 6(b). Figure 7(a) illustrates the variations of C, λ_1, load level, the numbers of void and solid elements with iteration number. In the iteration process, F is chosen as - 1MN initially. It can be seen that: 1) $\lambda_1 \rightarrow 1$ after iteration 33; 2) the maximum load level is F = -1.445 MN; 3) good convergences are achieved for these quantities in Figure 7(a). Figures 6 and 7(a) indicate the importance of introducing the buckling constraint in the optimization of geometrically nonlinear structures. Figure 7(b) illustrates the convergence histories of the iso-surface level (t) and compliance (C) in linear and nonlinear analyses. It is interesting to note that the fluctuation in t in the linear analysis is larger than that in the nonlinear analysis. After iteration 60, t and C are converged for linear and nonlinear cases.

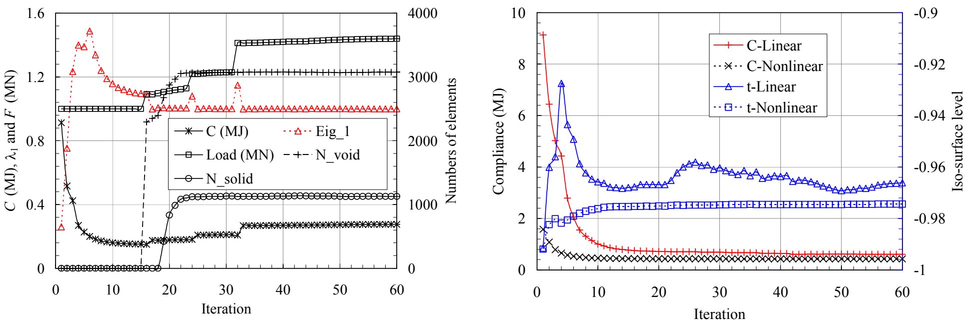

(a) Iterative process for nonlinear compliance (b) Variations of iso-surface level and compliance

Figure 7 (a) optimization for nonlinear compliance with the maximum load of -1.445 MN; (b) variations of t and C

4. Concluding remarks

Topology optimization for geometrically nonlinear compliance is re-defined as new formulation by removing void elements in FEA and introducing the buckling constraint. Numerical results show that the numerical issues in topology optimization for geometrically nonlinear structures can be resolved by excluding void elements in all nonlinear FEA and including them in the design variable update allowing reappearance of the material removed in previous iteration in the present MIST algorithm. By introducing a buckling constraint, optimal design can be obtained for geometrically nonlinear structures and the maximum load level without buckling can also be determined.

Acknowledgements

The authors are grateful for the support of the Australian Research Council via Discovery-Project Grants (DP140104408).

References:

[1] T. Buhl, C. B. W. Pedersen and O. Sigmund, Stiffness design of geometrically nonlinear structures using topology optimization, *Structural and Multidisciplinary Optimization,* **19** (2): 93-104, 2000.

[2] G. H. Yoon and Y. Y. Kim, Element connectivity parameterization for topology optimization of geometrically nonlinear structures, *International Journal of Solids and Structures,* **42** (7): 1983-2009, 2005.

[3] X. Huang and Y. M. Xie, Topology optimization of nonlinear structures under displacement loading, *Engineering Structures,* **30** (7): 2057-2068, 2008.

[4] T. E. Bruns and D. A. Tortorelli, An element removal and reintroduction strategy for the topology optimization of structures and compliant mechanisms, *International Journal for Numerical Methods in Engineering,* **57** (10): 1413-1430, 2003.

[5] R. Kemmler, A. Lipka and E. Ramm, Large deformations and stability in topology optimization, *Structural and Multidisciplinary Optimization,* **30** (6): 459-476, 2005.

[6] F. Wang, B. S. Lazarov, O. Sigmund and J. S. Jensen, Interpolation scheme for fictitious domain techniques and topology optimization of finite strain elastic problems, *Computer Methods in Applied Mechanics and Engineering,* **276** 453-472, 2014.

[7] G. I. N. Rozvany, Difficulties in truss topology optimization with stress, local buckling and system stability constraints, *Structural optimization,* **11** (3-4): 213-217, 1996.

[8] M. Zhou, "Topology optimization for shell structures with linear buckling responses," presented at the Computational Mechanics, WCCM VI, Beijing, China, 2004.

[9] M. Bruyneel, B. Colson and A. Remouchamps, Discussion on some convergence problems in buckling optimisation, *Structural and Multidisciplinary Optimization,* **35** (2): 181-186, 2008.

[10] E. Lindgaard and J. Dahl, On compliance and buckling objective functions in topology optimization of snap-through problems, *Structural and Multidisciplinary Optimization,* **47** (3): 409-421, 2013.

[11] P. A. Browne, C. Budd, N. I. M. Gould, H. A. Kim and J. A. Scott, A fast method for binary programming using first-order derivatives, with application to topology optimization with buckling constraints, *International Journal for Numerical Methods in Engineering,* **92** (12): 1026-1043, 2012.

[12] S. Uwe, Z. Ming, T. Poh-Soong and H. Cathal, "Topology Layout of Structural Designs and Buckling," in *10th AIAA/ISSMO Multidisciplinary Analysis and Optimization Conference*, ed: American Institute of Aeronautics and Astronautics, 2004.

[13] D. Manickarajah, Y. M. Xie and G. P. Steven, Optimisation of columns and frames against buckling, *Computers & Structures,* **75** (1): 45-54, 2000.

[14] L. Tong and J. Lin, Structural topology optimization with implicit design variable-optimality and algorithm, *Finite Elements in Analysis and Design,* **47** (8): 922-932, 2011.

[15] Q. Luo and L. Tong, Elimination of effects of low density elements on optimization for buckling structures, **(under review)**, 2014.

[16] Q. Luo and L. Tong, Eradication of effects of void elements on optimization for nonlinear compliance, **(under review)**, 2015.

[17] H. C. Gea and J. Luo, Topology optimization of structures with geometrical nonlinearities, *Computers & Structures,* **79** (20–21): 1977-1985, 2001.

[18] F. A. M. Gomes and T. A. Senne, An algorithm for the topology optimization of geometrically nonlinear structures, *International Journal for Numerical Methods in Engineering,* **99** (6): 391-409, 2014.

[19] Q. He, Z. Kang and Y. Wang, A topology optimization method for geometrically nonlinear structures with meshless analysis and independent density field interpolation, *Computational Mechanics,* **54** 629–644, 2014.

[20] R. D. Lahuerta, E. T. Simões, E. M. B. Campello, P. M. Pimenta and E. C. N. Silva, Towards the stabilization of the low density elements in topology optimization with large deformation, *Computational Mechanics,* **52** (4): 779-797, 2013.